Conformational Unfolding in the N-Terminal Region of Ribonuclease A Detected by Nonradiative Energy Transfer†

C. A. McWherter,‡ E. Haas,§ A. R. Leed,‡ and H. A. Scheraga*,‡

Baker Laboratory of Chemistry, Cornell University, Ithaca, New York 14853-1301, Department of Life Science, Bar-Ilan University, Ramat-Gan, Israel, and Chemical Physics Department, Weizmann Institute of Science, Rehovot, Israel

Received June 13, 1985; Revised Manuscript Received December 2, 1985

ABSTRACT: Unfolding in the N-terminal region of RNase A was studied by the nonradiative energy-transfer technique. RNase A was labeled with a nonfluorescent acceptor (2,4-dinitrophenyl) on the α-amino group and a fluorescent donor (ethylenediamine monoamide of 2-naphthoxyacetic acid) on a carboxyl group in the vicinity of residue 50 (75% at Glu-49 and 25% at Asp-53). The distribution of donor labeling sites does not affect the results of this study since they are close in both the sequence and the three-dimensional structure. The sites of labeling were determined by peptide mapping. The derivatives possessed full enzymatic activity and underwent reversible thermal transitions. However, there were some quantitative differences in the thermodynamic parameters. When the carboxyl groups were masked, there was a 5 °C lowering of the melting temperature at pH 2 and 4, and no significant change in $\Delta H(T_m)$. Labeling of the α-amino group had no effect on the melting temperature or $\Delta H(T_m)$ at pH 2 but did result in a dramatic decrease in $\Delta H(T_m)$ of the unfolding reaction at pH 4. The melting temperature did not change appreciably at pH 4, indicating that an enthalpy/entropy compensation had occurred. The efficiencies of energy transfer determined with both fluorescence intensity and lifetime measurements were in reasonably good agreement. The transfer efficiency dropped from about 60% under folding conditions to roughly 20% when the derivatives were unfolded with disulfide bonds intact and was further reduced to 5% when the disulfide bonds were reduced. The interprobe separation distance was estimated to be 35 ± 2 Å under folding conditions. The contribution to the interprobe distance resulting from the finite size of the probes was treated by using simple geometric considerations and a rotational isomeric state model of the donor probe linkage. With this model, the estimated average interprobe distance of 36 Å is in excellent agreement with the experimental result cited above.

Recent investigations (Lin et al., 1984, 1985) have suggested that the guanidine-induced unfolding of RNase A[1] proceeds sequentially with the N-terminal region unfolding before the rate-limiting step. This conclusion was based on a comparison of the thermodynamics and kinetics of the folding/unfolding of a cross-linked form of RNase A with those of the unmodified protein. In order to obtain further information about conformational unfolding in this localized region of the molecule, and hence about sequential unfolding, we have embarked on a series of experiments making use of nonradiative energy transfer (Steinberg, 1971; Stryer, 1978; Lakowicz, 1983) between small-molecule probes covalently attached to the surface of the protein in the N-terminal region.

Since the validity of the energy-transfer method (to determine the distance between the probes) depends on, among other things, the homogeneity of the protein, we present here the details and criteria for preparing a homogeneous protein sample and establishing the locations of the energy donor and acceptor groups. A nonfluorescent acceptor probe (DNP) was covalently attached to the α-amino group, and then a fluorescent donor (ENA) was covalently linked in the vicinity of residue 50 (75% at Glu-49 and 25% at Asp-53). The advantage of using a nonfluorescent acceptor is that all of the observed fluorescence can be assigned unambiguously to the donor probe. In addition, our analysis showed that, because the donor-labeled sites are close in both the amino acid sequence and the three-dimensional structure, the distribution of donor labels on two neighboring residues does not seriously affect the computed donor–acceptor distance.

In this initial study, we investigated the usefulness of this doubly labeled molecule for examining protein folding/unfolding by means of measurements of enzymatic actitivy, thermal-unfolding transitions, and energy transfer. A simple model was used to estimate the contribution of the probes to the average interprobe distance. This allowed a comparison of the two experimentally determined quantities, viz., the average interprobe distance (from energy-transfer results) and the distance between the points of attachment of the probes (from X-ray crystallographic results). This served to validate

† Based on the Ph.D. thesis of C.A.M., Cornell University, 1985. This work was supported by grants from the National Institute of General Medical Sciences (GM-14312), the National Science Foundation (DMB84-01811), and the U.S.–Israel Binational Science Foundation (BSF 2262/80). It was also supported in part by the National Foundation for Cancer Research.

‡ Cornell University.

§ Bar-Ilan University and Weizmann Institute of Science.

[1] Abbreviations: RNase A, bovine pancreatic ribonuclease A (EC 3.1.4.22); DNP, 2,4-dinitrophenyl; NAA, 2-naphthoxyacetic acid; ENA, ethylenediamine monoamide of NAA; α-DNP-RNase A, RNase A labeled on the α-amino group of Lys-1 with DNP; ENA-RNase A, RNase A labeled in the vicinity of residue 50 with one ENA group (see text for details); DNP-ENA-RNase A, α-DNP-RNase A labeled with one ENA group in the same manner as ENA-RNase A; SO_3, reduced and S-sulfonated protein; 2′(3′)Cp, cytidine 2′- and 3′-monophosphate (mixed isomers, sodium salt); 2′,3′-C>p, sodium salt of cytidine cyclic 2′,3′-phosphate; EPPS, *N*-(2-hydroxyethyl)piperazine-*N*′-3-propanesulfonic acid; HEPES, *N*-(2-hydroxyethyl)piperazine-*N*′-2-ethanesulfonic acid; Tris, 2-amino-2-(hydroxymethyl)-1,3-propanediol; FDNB, 1-fluoro-2,4-dinitrobenzene; HONSu, *N*-hydroxysuccinimide; NAA-ONSu, *N*-hydroxysuccinimide ester of NAA; DCC, dicyclohexylcarbodiimide; EDC, 1-ethyl-3-[3-(dimethylamino)propyl]carbodiimide hydrochloride; DTT, dithiothreitol; HPLC, high-performance liquid chromatography; RP-HPLC, reverse-phase HPLC.

0006-2960/86/0425-1951$01.50/0

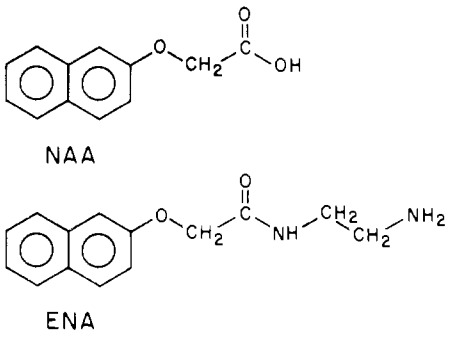

FIGURE 1: NAA, 2-naphthoxyacetic acid; ENA, ethylenediamine monoamide of 2-naphthoxyacetic acid.

the energy-transfer approach for our conformational unfolding studies of the N-terminal region of RNase.

Experimental Procedures

When two small organic molecules, one serving as a donor and the other as an acceptor of electronic excitation energy, are covalently attached to specific sites on a protein, then (provided certain conditions are met) the nonradiative transfer of energy by a dipole–dipole coupling mechanism can be used to estimate the distance between the donor–acceptor pair. For the transfer to occur, the emission spectrum of the donor must overlap with the absorption spectrum of the acceptor. Besides this spectral requirement, there are geometrical requirements for transfer; the emission and absorption dipoles of the donor and acceptor, respectively, must be in a certain distance regime and properly oriented for transfer to occur. Indeed, it is the dependence of the transfer efficiency E on the inverse sixth power of the distance that is used for estimating distances, viz.

$$E = R_0^6/(R_0^6 + r^6) \quad (1)$$

where r is the distance separating the pair and R_0 is a constant that depends on spectral and geometric factors of the system. The transfer efficiency is measured by fluorescence intensity and/or fluorescence lifetimes (Fairclough & Cantor, 1978; Lakowicz, 1983).

Thus, the selection of the probes takes the following factors into account: proper amount of spectral overlap for the distance range of interest, no perturbation of the conformation, insensitivity to changes in environment (e.g., polarity), a low degree of polarization to reduce the effect of orientation, a large Stokes shift for the donor probe to facilitate suppression of scattered exciting radiation, and convenient chemistry for covalent attachment to a single site or, at least, to a limited number of sites. The final selection inevitably represents a compromise between all of these factors.

Preliminary results with derivatives of 2-naphthoxyacetic acid (E. Haas, unpublished results; Amir et al., 1985) indicated that this chromophore would be useful in light of the above considerations. In particular, it would allow for excitation at wavelengths longer than the tyrosine absorption band and has an emission maximum (~340 nm) that overlaps substantially with the nonfluorescent acceptor DNP. Therefore, a donor probe was synthesized by coupling an ethylenediamine linker arm to 2-naphthoxyacetic acid (NAA, see Figure 1). The free amino group of the resulting ethylenediamine monoamide of naphthoxyacetic acid (ENA, see Figure 1) was then available for coupling to protein carboxyl groups with a water-soluble carbodiimide.

Materials. RNase A (type IIA), a mixture of cytidine 2′- and 3′-monophosphate [2′(3′)Cp], ε-DNP-Lys·HCl, EPPS, HEPES, and Tris were obtained from Sigma Chemical Co., St. Louis, MO. The RNase A was purified further by chromatography on a carboxymethylcellulose (CMC) column (CM-52, Whatman, Inc., Clinton, NJ) according to the method of Taborsky (1959). 1-Fluoro-2,4-dinitrobenzene (FDNB) was purchased from Pierce Chemical Co., Rockford, IL. NAA was obtained from Aldrich Chemical Co., Milwaukee, WI, and was crystallized first from 2:1 ethanol–water and then from benzene. N-Hydroxysuccinimide (HONSu) was obtained from Aldrich and crystallized from ethyl acetate. Dicyclohexylcarbodiimide (DCC), from Eastman Kodak Co., Rochester, NY, and ethylenediamine (Gold label grade), from Aldrich, were used without purification. Tetrahydrofuran (THF), obtained from Fisher Scientific Co., Pittsburgh, PA, was stored over activated 3-Å molecular sieves at 0 °C in the dark. Dimethylformamide (DMF) was distilled under reduced pressure in a nitrogen atmosphere and stored over activated 3-Å molecular sieves. Immediately before use, volatile amines were removed by bubbling nitrogen through the DMF. Ac-Asp(OBzl)-$NHCH_3$ was a gift from Dr. Evelyn R. Stimson. ENA and Ac-Asp(ENA)-$NHCH_3$ were prepared as described below and in the supplementary material (see paragraph at end of paper regarding supplementary material). All other solvents and reagents were analytical grade and were used as purchased.

Preparation of ENA. ENA was formed by the reaction of ethylenediamine with the *N*-hydroxysuccinimide ester of NAA. The details of the preparation and characterization of the product are available in the supplementary material.

Preparation of α-DNP-RNase A. The procedure used to prepare α-DNP-RNase A is based on the work of Hirs et al. (1965). FDNB was reacted with RNase A in the presence of the inhibitor 2′(3′)Cp, which served to prevent reaction with the ε-amino group of Lys-41. After removal of excess FDNB, the protein solution was desalted, and the products were fractionated by cation-exchange chromatography, first at pH 7 and then again at pH 8. The procedure began with 1.2 g of purified RNase A, and nearly 150 mg of α-DNP-RNase A was recovered for an overall yield of 12%. Details concerning the preparation and purification of this product are in the supplementary material. Further characterization of this product is described below.

Preparation of ENA-RNase A. The amino group of ENA was coupled to carboxylate groups on the protein with a water-soluble carbodiimide at pH 4.75. The details of the preparation can be found in the supplementary material. Briefly, a large excess of ENA was combined with RNase A in EtOH as a cosolvent. The pH of the solution was adjusted to 4.75 and maintained at this value throughout the course of the reaction. The water-soluble carbodiimide EDC was then added. The reaction was arrested, and the excess reagents and byproducts were removed. After lyophilization, the product was redissolved and purified by chromatography on a CMC cation-exchange column at pH 7 and an HPLC cation-exchange column (Mono S) at pH 4.5. The procedure began with 400 mg of RNase A and gave an overall yield of 15%.

Preparation of DNP-ENA-RNase A. Reaction conditions for the preparation of DNP-ENA-RNase A were identical with those for ENA-RNase A described in the preceding section and in the supplementary material except that α-DNP-RNase A was substituted for RNase A. The product was purified by chromatography on CMC columns, first at pH 7 and then at pH 8. The chromatographic procedure is presented in detail in the supplementary material.

Analytical-Scale Cation-Exchange HPLC. All of the derivatives studied were subjected to analytical-scale cation-

exchange HPLC as a test of homogeneity under conditions described in the legend of Figure 2.

Peptide Mapping. Procedures and conditions for peptide mapping were the same as those previously described (McWherter et al., 1984; Thannhauser et al., 1985). Peptides containing the DNP group were detected by absorbance at 360 nm, and peptides containing the ENA group were detected on a Kratos Model FS-950 fluorescence detector. Excitation made use of a chemical band-pass filter (Kasha, 1948) centered at 313 nm, and emission was detected above 340 nm by means of a long-pass cut-off filter.

Activity Measurements. Enzymatic activity measurements of the various derivatives relative to unmodified RNase A were made spectrophotometrically on a modified Cary Model 14 spectrophotometer (Denton et al., 1982) and with cytidine cyclic 2′,3′-phosphate (2′,3′-C>p) as the substrate (Crook et al., 1960). All activity measurements were made in triplicate as was the determination of protein concentrations by micro-Kjeldahl nitrogen analysis (Noel & Hambleton, 1976).

Extinction Coefficients. Extinction coefficients of the derivatives were determined by measuring the UV-absorption spectra with the modified Cary Model 14 and independently determining the concentration by either micro-Kjeldahl nitrogen analysis (Noel & Hambleton, 1976) or quantitative amino acid analysis on the Waters Associates (Milford, MA) Pico-Tag system.

Thermal Transition Curves. The reversible thermal transitions from the folded state to the thermally unfolded state were recorded spectrophotometrically for all the derivatives studied here (α-DNP-RNase A, ENA-RNase A, and DNP-ENA-RNase A) and for unmodified RNase A by the procedures commonly employed (Hermans & Scheraga, 1961; Brandts & Hunt, 1967; Konishi & Scheraga, 1980). UV-difference spectra between the folded state and the thermally unfolded state for all derivatives used in this study appeared qualitatively the same as that of unmodified protein with a maximum around 287 nm (Figure 3). This indicates the suitability of absorption measurements at 287 nm for following the thermal transitions of these derivatives.

The transitions were recorded in stoppered, small-volume (1.5-mL) quartz cells that had black masking to reduce stray light (type 29M, NSG precision cells). Starting at about 5 °C, the sample was allowed to equilibrate thermally (10–15 min), and then the absorbance at 287 nm was recorded. The temperature was regulated to within 0.1 °C by means of an external bath (Haake, type F) and was determined to within 0.1 °C by means of a calibrated thermistor dipped into a quartz cell that was placed adjacent to the sample cell. The temperature was then increased, and after thermal equilibration, the absorbance and temperature were recorded. This procedure was repeated throughout the heating curve with 4–5 °C intervals outside the transition and 1–2 °C intervals inside the transition zone. The cooling curves were obtained by reversing the procedure. It was found necessary to minimize the exposure to high temperature (no more than 15 min at each temperature) in order to obtain suitably reversible transition curves.

Fluorescence Emission Spectra. Fluorescence emission spectra were recorded on a Perkin-Elmer Model MPF-44B spectrofluorometer in the energy mode. The concentration of all samples used in making fluorescence measurements was adjusted to give an absorbance below 0.005 (at the wavelength of maximum absorbance) so that deviations due to the innerfilter effect and reabsorption could be neglected. The spectra of blanks and a standard consisting of Ac-Asp-(ENA)-$NHCH_3$ were recorded immediately before and after each series of measurements. In all cases, no appreciable drift was observed. A small amount of background fluorescence in Gdn·HCl solutions did not make an appreciable contribution at the wavelengths used in this study. Corrected emission spectra were recorded with the above instrument and a DSCU-2 spectral correction unit. Emission spectra were digitized and stored on a Prime 550 minicomputer using an MM1103 series digitizing pad (Summagraphics Corp., Fairfield, CT).

Fluorescence polarization spectra were recorded on a Perkin-Elmer MPF-44B spectrofluorometer. A standard of rhodamine in pure glycerol (at ambient temperature) gave a value of 0.43 [lit. value 0.46, in 95% glycerol at 10 °C (Chen & Bowman, 1965)]. Samples studied included ENA in glycerol and ENA-RNase A in both glycerol and water at ambient temperature.

Steady-State Energy-Transfer Measurements. Steady-state energy-transfer measurements were made by comparing the intensity of fluoroescence at 342 nm of a sample of ENA-RNase A excited at either 295 or 315 nm to that of DNP-ENA-RNase A under the same conditions. The amount of energy transfer was identical (±1%) at the two wavelengths, thus demonstrating that the solvent Raman band does not interfere with these measurements. Usually, the concentrations of both samples were adjusted to be identical by appropriate dilution of stock solutions whose concentrations were determined spectrophotometrically. In some experiments, the dilutions were made so that the concentrations of the two samples were not identical. For these samples, the concentrations were determined by quantitative amino acid analysis. The concentrations were adjusted so that the innerfilter effect and reabsorption could be ignored (see above). In all cases, the determination of the efficiency of energy transfer was made by comparison of the samples under identical solution conditions (e.g., pH, with or without Gdn·HCl, etc.).

The efficiency of energy transfer E from intensity measurements was calculated according to (Fairclough & Cantor, 1978)

$$E = 1 - F_{DA}C_D/(F_DC_{DA}) \quad (2)$$

where F_{DA} and F_D are the donor fluorescence of the doubly labeled and donor-labeled samples, respectively, and C_{DA} and C_D are the concentrations of the doubly labeled and donor-labeled samples, respectively.

Lifetime Measurements. Fluorescence lifetime measurements were made on an instrument based on the pulse-sampling technique, as described previously (Hundly et al., 1967; Hazan et al., 1974; Hazan, 1973). Corrections due to Rayleigh and Raman scattering and due to background fluorescence were made as described before (Haas et al., 1978b). The lifetimes were determined by using a nonlinear least-squares analysis of the fluorescence decay kinetics (Grinvald & Steinberg, 1974). Both nitrogen and deuterium flashlamps (TRW, Inc., Torrance, CA) were used for excitation. The excitation pulse was selected either by means of a Jarrel-Ash double monochrometer or with a chemical band-pass filter (Kasha, 1948) centered at 313 nm.

The efficiency of energy transfer from lifetime measurements was calculated according to

$$E = 1 - \tau_{DA}/\tau_D \quad (3)$$

where τ_D and τ_{DA} are the donor fluorescence lifetimes of the donor- and double-labeled protein, respectively, independent of concentration.

Overlap Integrals, Quantum Yields, Refractive Indices, R_0, and r (Lakowicz, 1983). The overlap integral J was calculated according to the equation

$$J = \frac{\int F_D(\lambda)\epsilon_A(\lambda)\lambda^4\, d\lambda}{\int F_D(\lambda)\, d\lambda} \quad (M^{-1}\ cm^3) \qquad (4)$$

where F_D is the corrected fluorescence emission spectrum of the donor-labeled protein, ϵ_A is the molar extinction coefficient of the acceptor-labeled protein, and λ is the wavelength in centimeters.

The quantum yield Q_D was determined for ENA-RNase A in H_2O at pH 6 with the comparative method and the equation (Chen, et al., 1969)

$$Q_D = Q_{Std}\frac{A_{Std}\int F_D(\lambda)\, d\lambda}{A_D\int F_{Std}(\lambda)\, d\lambda} \qquad (5)$$

F_{Std} is the corrected fluorescence emission of the standard, Q_{Std} is its quantum yield, and A_D and A_{Std} are the absorbances of ENA-RNase A and the standard, respectively, at the wavelength of excitation. The polarization correction to the quantum yields (Weber & Teale, 1957) are negligible because of the Brownian rotational motion of the donor in the low-viscosity solvent; the polarization of ENA-RNase A was 0.05, and that of free napthalene is undoubtedly smaller. The quantum yields under other solvent conditions were estimated from lifetime measurements and the relation

$$Q_1/Q_2 = \tau_1/\tau_2 \qquad (6)$$

where the τ's and Q's are the lifetimes and quantum yields, respectively. The subscript 1 refers to the reference condition (H_2O, pH 6), and the subscript 2 refers to the conditions for which the quantum yield is to be determined. Zone-refined naphthalene (kindly donated by Dr. Z. Ludmir of the Weizmann Institute of Science) was used as the standard (Berlman, 1971).

The refractive indices n of the buffers used for energy-transfer measurements were determined with an Abbe refractometer (Bausch and Lomb Optical Co., Rochester, NY). The measurements, corresponding to the values at the sodium D line, are relatively insensitive to wavelength in the range used in these studies. These values were used in the calculations of R_0 and also for determining the concentrations of Gdn·HCl solutions (Nozaki, 1972).

R_0, the distance at which 50% of the excitation energy is transferred, was calculated from

$$R_0 = (9.79 \times 10^3)(\kappa^2 n^{-4} J Q_D)^{1/6}\ (Å) \qquad (7)$$

where κ^2 is a parameter related to the mutual orientation of the probes and all other variables have been defined previously. The value of κ^2 was taken as $^2/_3$ (see Results and Discussion). The separation distance r between the donor–acceptor pair was calculated from eq 1.

Results and Discussion

Preparation of α-DNP-RNase A. The preparation and identification of α-DNP-RNase A has been reported previously (Hirs et al., 1965; Hirs & Kycia, 1965; Murdock et al., 1966). These workers found that 3 of the 11 amino groups of RNase A (the α-amino group of Lys-1 and the ε-amino groups of Lys-7 and Lys-41) have enhanced reactivity toward FDNB. They also observed that the use of a mixture of inhibitors [2′(3′)Cp] effectively prevented reaction of Lys-7 and Lys-41.

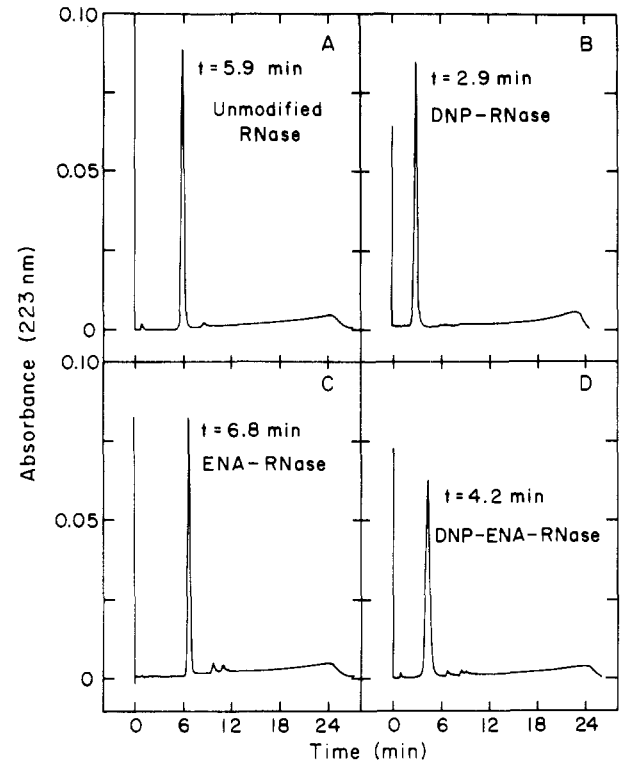

FIGURE 2: Homogeneity of α-DNP-RNase A, ENA-RNase A, and DNP-ENA-RNase A assessed by analytical-scale cation-exchange HPLC. The protein samples were chromatographed on a Mono S HR 5/5 column equilibrated with 50 mM sodium phosphate, pH 7. A linear gradient from 0 to 400 mM NaCl in 20 min was employed with a flow rate of 1 mL/min. About 30 μg of each protein were injected, and the effluent was monitored at 223 nm. The elution times of the major components are shown.

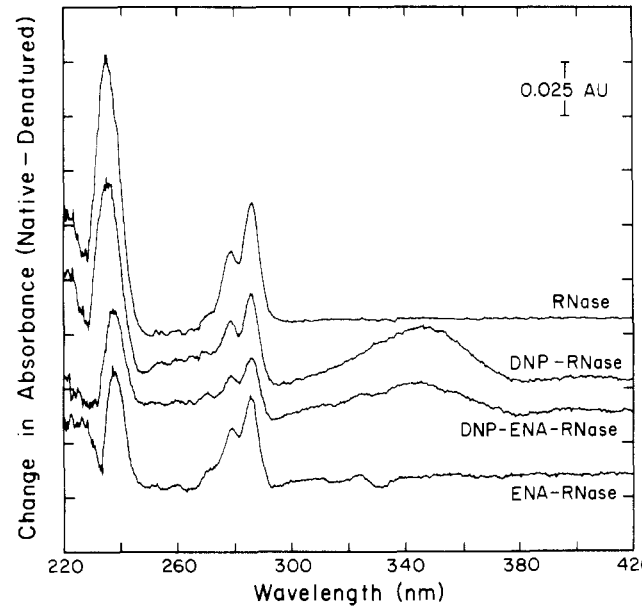

FIGURE 3: Thermal difference spectra of RNase A and derivatives of RNase A. The difference spectra (native – denatured) were recorded in 50 mM Gly-HCl, pH 1.97, under the following conditions: RNase A, 24 μM, 6.2–52.1 °C; α-DNP-RNase A, 21 μM, 7.0–54.3 °C; DNP-ENA-RNase A, 13 μM, 6.0–38.0 °C; ENA-RNase A, 20 μM, 5.5–43.1 °C. The ordinates of the curves were shifted in order to present all four spectra in a single figure. The characteristic double maxima around 278 and 287 nm, due to the change in polarity of the environment of the tyrosyl side chains, is evident.

We have made use of these facts to increase the yield of α-DNP-RNase A and to eliminate the favored product, 41-ε-DNP-RNase A.

Table I: Summary of Some Properties of Labeled RNases

sample	ϵ_{275}[a]	ϵ_{295}[a]	act.[b]	$\Delta\epsilon_{287}$[c]	λ_{max}[d]	T_m(pH 2)[e]	$\Delta H(T_m$,pH 2)[f]	T_m(pH 4)[g]	$\Delta H(T_m$,pH 4)[f]
native	9800	300	100.0	1900[h]	286.0	29.0 ± 0.2[i]	60 ± 2[j]	54.3 ± 0.2[k]	103 ± 4[l]
DNP-RNase A	16500	4000	99.6	1600	286.3	29.2 ± 0.2	55 ± 3	53.4 ± 0.3	77 ± 4
ENA-RNase A	14600	1350	99.7	1600	285.5	22.8 ± 0.2	57 ± 4	49.7 ± 0.2	96 ± 5
DNP-ENA-RNase A	23450	4750	100.0	1650	286.0	23.3 ± 0.2	60 ± 2	48.9 ± 0.4	71 ± 6

[a] Extinction coefficient (M^{-1} cm^{-1}) using concentration of stock solutions in H_2O determined by nitrogen analysis. The dilution buffer was 50 mM Gly·HCl, pH 1.97. The contributions from the protein, DNP, and ENA are additive to within 10%. [b] Enzymatic activity relative to native. Activity is initial velocity/concentration (Crook et al., 1960). [c] Difference (native − denatured) in extinction coefficient (M^{-1} cm^{-1}) at 287 nm. Buffer was 50 mM Gly·HCl, pH 1.97. [d] Wavelength (nm) of maximum difference in extinction coefficient between native and thermally denatured protein. [e] T_m (°C) is obtained from the temperature at which ln K_D = 0 in the van't Hoff plot. Buffer was 50 mM Gly·HCl, pH 1.97. [f] $\Delta H(T_m)$ (kcal/mol) determined from the van't Hoff plot. [g] Same as footnote *e* except that buffer was 100 mM potassium acetate, pH 3.93, with sufficient KCl added to give an ionic strength of 200 mM. [h] Literature: 1600 M^{-1} cm^{-1}, pH 2.10, unbuffered (Brandts & Hunt, 1967). [i] Literature: 28 °C, 50 mM Gly·HCl, pH 2 (Lin et al., 1984). [j] Literature: 64 kcal/mol, 50 mM Gly·HCl, pH 2 (Lin et al., 1984). [k] Literature: 54.3 °C, 100 mM Tris–acetate, pH 4 (Lin et al., 1984). [l] Literature: 99 kcal/mol, 100 mM Tris–acetate, pH 4 (Lin et al., 1984).

The enzyme was first incubated with an excess of the inhibitor 2′(3′)Cp and then reacted with FDNB. The reaction products were fractionated on successive CMC columns at pH 7 and pH 8. Amino acid analysis of the product (results not shown) indicated that it was dinitrophenylated, on average, at one lysyl residue per mole of protein. Analytical-scale cation-exchange HPLC (Figure 2B) demonstrated that the product was chromatographically homogeneous. A tryptic peptide map of an S-sulfonated sample of the product was obtained as described by Thannhauser et al. (1985). A single dinitrophenylated peptide, corresponding to the amino-terminal sequence Lys-Glu-Thr-Ala-Ala-Ala-Lys, was detected by absorbance at 365 nm. It follows that the product is labeled at Lys-1 since labeling at Lys-7 would have prevented tryptic cleavage after Lys-7 and this peptide would not have been observed. The DNP group was further localized to the α-amino group of Lys-1 by HPLC anion-exchange of an acid hydrolysate of the product (results not shown). The elution position of the single 365-nm peak was consistent with α-DNP-Lys and quite different from a commercial sample of ε-DNP-Lys.

In summary, a combination of chromatographic mobility, UV-absorption measurements, amino acid analysis, peptide mapping, and HPLC anion-exchange demonstrates that the site of dinitrophenylation is the α-amino group. Further details regarding the assignment of the product as α-DNP-RNase A are provided in the supplementary material. This result is in complete agreement with previous results (Hirs et al., 1965; Hirs & Kycia, 1965; Murdock et al., 1966). Further characterization of this product is described below.

Preparation of ENA-RNase A. The amino group of ENA was coupled to RNase A by using EDC (Riehm & Scheraga, 1966; Carraway & Koshland, 1972). This reaction increases the net positive charge of the protein, thereby making it possible to fractionate the reaction products on a cation-exchange column. One of the peaks from the CMC column (see supplementary material for the full details of the purification) had a chromatographic mobility and a UV absorption indicative of a monosubstituted product. This product subsequently split into two monosubstituted species when chromatographed on a cation-exchange HPLC column at pH 4.5. The peak recovered in highest yield was retained for further study.

A comparison of the UV-absorption profile of the model compound N-Ac-Asp(ENA)$NHCH_3$ with the purified material (results not shown) revealed that they were nearly identical above 290 nm with both exhibiting peaks at 311 and 325 nm. A sample of this material was subjected to analytical-scale cation-exchange HPLC (Mono S) at pH 7, as shown in Figure 2C, and was found to be chromatographically homogeneous. Furthermore, rechromatography on cation-exchange HPLC at pH 4.5 (results not shown) gave a single peak, providing further evidence of homogeneity. Thus, the product is monolabeled with ENA and is chromatographically homogeneous and will hereafter be designated as ENA-RNase A.

Peptide mapping of ENA-RNase A revealed that it was actually a mixture of monolabeled species with about 75% of the molecules monolabeled at Glu-49 and the remainder monolabeled at Asp-53. This was deduced from amino acid compositions of ENA-containing peptides obtained from tryptic–chymotryptic RP-HPLC peptide maps of ENA-RNase A. The ENA-containing peptides were identified from the characteristic spectral properties (absorbance or fluorescence) of the ENA group. There were two major ENA-containing peptides observed (residues 52–55 and residues 47–55). The final determination of the labeling distribution, however, required a more complicated analysis; this analysis is set forth in the supplementary material.

As further evidence, the analysis of the peptide map of DNP-ENA-RNase A (see below) unambiguously showed the same labeling distribution. This distribution is acceptable for the present studies for reasons given below.

Preparation of DNP-ENA-RNase A. The preparation of double-labeled RNase A paralleled the preparation of ENA-RNase A in most respects. The initial fractionation took place on a CMC column at pH 7. An elution pattern very similar to that obtained from the labeling of RNase A was observed. The product, chosen on the basis of mobility, was rechromatographed on a CMC column at pH 8. A peak was recovered and shown to be chromatographically homogeneous by analytical-scale HPLC (Figure 2D). This material, which we designate as DNP-ENA-RNase A, is labeled with one ENA group per mole of protein on the basis of its chromatographic mobility. This statement is based on the close similarity of the pH 7 CMC elution profiles of the ENA-RNase A and DNP-ENA RNase A fractionations.

The site(s) of attachment of the ENA group was (were) determined by a tryptic–chymotryptic peptide map monitored specifically for the ENA group by fluorescence detection. Amino acid analysis of the two ENA-containing peptides observed revealed a labeling distribution of 75% at Glu-49 and 25% at Asp-53. Thus, within experimental error, DNP-ENA RNase A has the same labeling distribution as ENA-RNase A. Further information on this assignment will be found in the supplementary material. This particular product distribution for DNP-ENA-RNase A is acceptable for the present studies for reasons presented below.

Suitability of the Derivatives for Protein Folding Studies. To interpret the results of folding studies of these derivatives by the energy-transfer technique, independent verification that they fold reversibly to a native-like conformation is required. For this purpose, the derivatives were characterized further

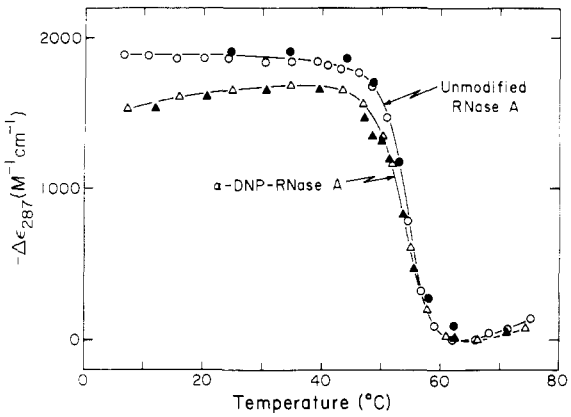

FIGURE 4: Thermal transition curves. Unmodified RNase A, 24 μM, in 100 mM potassium acetate, pH 3.93 [(○) heating; (●) cooling], and α-DNP-RNase A, 65 μM, in the same buffer [(△) heating; (▲) cooling].

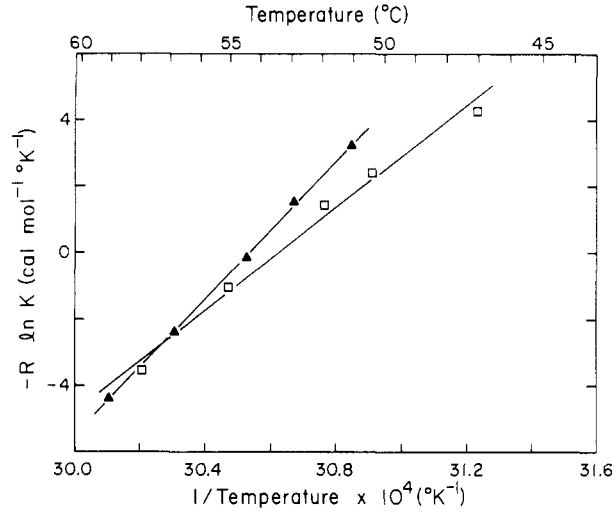

FIGURE 5: van't Hoff plots. $-R \ln K$ is plotted against $1/T$, where K is the equilibrium constant for the unfolding reaction. Values of K only within the limits $0.1 \leq K \leq 10$ are used. The definition and evaluation of K conform to accepted protocol (Brandts, 1964). The thermal transitions of unmodified RNase A (▲) and α-DNP-RNase (□) (from Figure 4) were analyzed. The solid lines represent least-squares fits to the points, and the slopes give the value of ΔH.

by their UV spectra, enzymatic activity, and reversible thermal unfolding. The results are summarized in Table I and are analyzed below.

Enzymatic Activity as a Gauge of Conformational Integrity. Whenever extrinsic probes are covalently attached to a protein, it is necessary to evaluate the effect on the conformation. Measurement of enzymatic activity is a highly sensitive method for detecting conformational perturbations. The maintenance of active site geometry requires the correct spatial juxtaposition of several functional groups that are often widely separated in the linear sequence. Thus, the requirement that His-12, Lys-41, and His-119, among others, form the active site of RNase A (Richards & Wyckoff, 1971; Blackburn & Moore, 1982) implies that significant deviations from the native conformation anywhere in the sequence are likely to alter the observed activity.

All of the derivatives were found to be fully active toward the substrate 2',3'-C>p (Table I). The uncertainty in these results is estimated to be 5%. This demonstrates that all of the derivatives studied here maintain the native conformation under folding conditions. Also, ENA-RNase A and DNP-ENA-RNase A exhibited full enzymatic activity after thermal unfolding and cooling at pH 4 (see below) provided that the time spent under unfolding conditions was minimized. Thus, neither the donor nor acceptor prevent readoption of the native conformation after thermal unfolding.

Other workers (Riehm & Scheraga, 1966; Acharya & Vithayathil, 1975) have found that RNase A modified at Asp-53 possesses full activity, and our results are in agreement with these earlier observations. Hirs (Hirs et al., 1965) found that α-DNP-RNase A possessed only 60% activity. The reason for the discordance with our results is unknown, but we would suggest that our inclusion of an inhibitor, which prevented reaction at Lys-41, led to a more homogeneous derivative and, hence, to the observed higher activity. Other reports of nearly full activity for α-amino derivatives of RNase A have appeared (Carty & Hirs, 1968; Matheson et al., 1977; Garel, 1976).

Thermal Unfolding of the Labeled RNase. The first important result from the thermal unfolding studies was that all three derivatives (α-DNP-RNase A, ENA-RNase A, and DNP-ENA-RNase A) exhibited reversible thermal transitions at pH 2 and 4. As an example, Figure 4 illustrates the thermal transitions of unmodified RNase and α-DNP-RNase A. In all cases, there was a close correspondence between the heating and cooling curves, provided that the time that the samples were exposed to temperatures above the melting temperature (T_m) was minimized (Hermans & Scheraga, 1961). Figure 5 shows, as an example, the van't Hoff analysis of the above two thermal transitions.

First, we concentrate on the effect of masking the carboxyl group (in a ratio of 3:1, Glu-49 to Asp-53). At pH 2, comparison of the unmasked derivatives (unmodified RNase and α-DNP-RNase A) with the masked ones (ENA- and DNP-ENA-RNase A) reveals a depression in the value of T_m of 5–6 °C. The change in enthalpy, $\Delta H(T_m)$, upon unfolding remains the same to within experimental error. The same result is obtained at pH 4, although the situation is complicated by the influence of the DNP group on the denaturation thermodynamics at this pH (see below). Nevertheless, comparison at pH 4 of unmodified RNase A to ENA-RNase A and α-DNP-RNase A to DNP-ENA-RNase A reveals the same pattern, that is, a 5 °C depression of T_m and a relatively invariant $\Delta H(T_m)$. This is in agreement with the results of Riehm and Scheraga (1966), who found that modification of Asp-53 lowered T_m by about 5 °C between pH 2 and pH 6. They interpreted their results in terms of a general loosening of the structure as carboxyl groups became progressively modified. This trend correlated roughly with loss of enzymatic activity, although the derivative with Asp-53 modified did retain full activity.

We now turn our attention to the effect of the labeling of the α-amino group with DNP. At pH 2, the DNP group has little or no effect on either T_m or $\Delta H(T_m)$. At pH 4, however, there is a dramatic decrease in $\Delta H(T_m)$ ($\sim$25 kcal/mol) of the transition. It was quite surprising to find such a large reduction in $\Delta H(T_m)$ given the lack of intramolecular contact between the α-amino group and the rest of the protein (Wlodawer et al., 1982). Nevertheless, we considered the possibility that the DNP group was influencing interactions normally present in the native structure. To investigate this, the unfolding transition of α-DNP-RNase A at pH 2 was monitored at 350 nm. The results (Figure 6) give no evidence for a cooperative change in the environment of the DNP group.

The strongest conclusion we can draw is that, at pH 4, the DNP group reduces the enthalpy change of the transition but that the T_m remains unchanged, presumably because of an entropic compensation. The difference in results at pH 2 and pH 4 may suggest the interaction of the α-amino group with

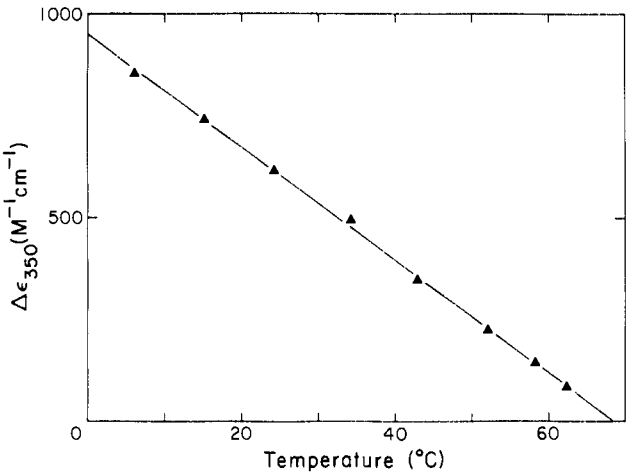

FIGURE 6: Thermal unfolding of α-DNP-RNase A monitored by the absorbance of the DNP group. The thermal unfolding of α-DNP-RNase A, 21 μM, was monitored at 350 nm, which is the wavelength of maximum difference for the DNP group (see Figure 3). A linear change in the extinction coefficient is observed. The change was arbitrarily made with reference to the value at 62 °C. The solid line is a least-squares fit, which gave a slope of -16.7 M^{-1} cm^{-1} $°C^{-1}$.

a group(s) important for the steepness of the transition that titrate(s) between pH 2 and pH 4.

Determination of R_0. In general, the variables that enter into the calculation of R_0 (eq 7) will depend on the solution conditions under which they are determined (i.e., pH, Gdn·HCl, etc.). For this reason, R_0 was calculated for each condition studied by making separate determinations of J, Q, and n (see Experimental Procedures).

A value of $^2/_3$ was adopted for κ^2 in these calculations under the assumption of a random distribution of the mutual orientations of the probes. The value of κ^2 can range between 0 and 4. The error in R_0 and r introduced by the assumption that $\kappa^2 = {}^2/_3$ becomes large when the true value of κ^2 approaches 0. There are two reasons why this assumption is unlikely to introduce large errors. First, this assumption is plausible because of the partial rotational freedom around each of the six single bonds in the linker arm that attaches the aromatic portion of the probe to the protein (Figure 1). The rotational motion of the donor probe superimposed upon that of the protein will result in a cumulative depolarization of the fluorescence (Soleillet, 1929; Lakowicz & Weber, 1980). According to Lakowicz and Weber (1980), these effects are accounted for by using the equation

$$d = d_t d_p \tag{8}$$

where d, d_t, and d_p are the depolarization ratios due to the overall rotation, the rotation of the probe, and the rotation of the protein, respectively. The depolarization ratio is defined by

$$d = r/r_0 \tag{9}$$

where r is the anisotropy and the subscript zero indicates the anisotropy under limiting conditions. The value of d is thus calculated from the polarization of ENA-RNase fluorescence under viscous (r_0) and nonviscous (r) conditions. The polarization of ENA-RNase A at room temperature was 0.05 in water and 0.28 in glycerol. This compares well with the value for ENA in glycerol of 0.30 (see below). The value of d_p can be calculated from the Perrin equation with a rotational correlation time of 7.2 ns for RNase A from electric birefringence data (Richards & Wyckoff, 1971) and an excited-state lifetime of 13.4 ns. The value of d_t is then easily calculated with eq 8. This may be converted to the polarization p_t, which is due to the rotation of the probe relative to the protein. The result of this calculation gives $p_t = 0.14$, and the Perrin equation yields a rotational correlation time of 10.4 ns for the donor relative to the protein. Clearly, the fluorescence is depolarized by the motion of the probe during the lifetime of the excited state. The Perrin equation assumes spherical symmetry and, therefore, does not distinguish faster anisotropic motion (Thomas, 1978). Nevertheless, the donor does have significant dynamic averaging while it is in the excited state. The fluorescence decay of ENA-RNase A, which is monoexponential with the same lifetime as the model compounds both in the folded and unfolded state, further supports this conclusion. It shows that there appear to be no specific interactions of the aromatic chromophore with the protein side chains or backbone and that the probe is relatively free to rotate.

It is also quite likely that the acceptor would rotate rapidly about the N–C bond connecting it to the protein within the lifetime of the excited state. First, the DNP group is an extension of the α-amino group, which is known to be chemically reactive and solvent accesible. The X-ray structure supports the view that the DNP group would extend into the solvent away from the protein. Second, the results of the thermal transitions do not support the suggestion of an immobilized DNP group. If the DNP group were immobilized by interacting strongly with the protein, then one might expect to see this manifested in the T_m of the unfolding equilibrium and/or the observation of a cooperative phenomenon when the transition was monitored by the DNP group absorbance. Neither of these effects was observed. This rotation would further average the relative orientations of the probes.

Large errors in R_0 due to the assumed value of the orientation factor are also less likely because of the nature of the electronic transitions of ENA. The limiting polarization of ENA in frozen solution (pure glycerol), when excited on the red-edge of the longest wavelength band, gave a moderate value of 0.30. This indicates that there is a mixed polarization of the electronic transitions of ENA (E. Haas, unpublished results; Haas et al., 1978a). A pair of related chromophores (1- and 2-naphthylamine) has been shown to have multiple transitions that contribute to the emission (Valeur & Weber, 1977, 1978). This, taken together with the limiting polarization, suggests that emission arises from transitions of mixed polarization. We have no information about the polarization of the electronic transitions of the DNP acceptor chromophore since it is not fluorescent. The effect of the orientation of the donor and acceptor on the probability of energy transfer involving electronic transitions of mixed polarization has been treated by Steinberg and co-workers (Haas et al., 1978a). Considering a p_t of 0.14, even if the acceptor has a single transition dipole in the spectral range overlapping the ENA emission, the maximal uncertainty introduced by taking κ^2 as $^2/_3$ is not larger than 20% in frozen solution [see Table II of Haas et al. (1978a)]. Most experiments were carried out in nonviscous buffers in which the orientation of the acceptor dipole will be dynamically averaged (see arguments presented above). In this case, the uncertainty in R_0 introduced by assuming $\kappa^2 = {}^2/_3$ is less than 10% [Table II in Haas et al. (1978a)].

It is pertinent to note that the decay of the fluorescence of the ENA donor chromophore in the doubly labeled DNP-ENA-RNase A in the native state is, within experimental error, reasonably well represented by a monoexponential decay and a single distance. This further supports the use of a single average value of κ^2. The decay is not perfectly monoexpo-

Table II: Summary of Energy Transfer and Related Results

sample[a]	solvent[b]	τ (ns)[c]	max dev[d]	RMS[e]	n[f]	$J \times 10^{14}$ (M^{-1} cm^3)	Q	R_0 (Å)	% $E(I)$[g]	% $E(\tau)$[h]	$r(I)$[i]	$r(\tau)$[j]
Asp(ENA)	pH 2	12.9	0.018	0.0090[k]								
D	pH 2	12.1	0.009	0.0032	1.3339	2.26	0.55	36.4	62	45	33.5	37.6
DA	pH 2	6.6	0.027	0.0128								
Asp(ENA)	pH 4	13.1	0.0167	0.0070[k]								
D	pH 4	13.4	0.0121	0.0041	1.3352	2.35	0.61	37.2	64	61	33.8	34.5
DA	pH 4	5.2	0.0157	0.0050								
Asp(ENA)	pH 4/Gdn·HCl	9.4	0.0151	0.0060[k]								
D	pH 4/Gdn·HCl	9.3	0.0069	0.0025	1.4431	2.36	0.42	33.2	19	18	42.3	42.7
DA	pH 4/Gdn·HCl	7.6	0.0398	0.0111								
D	pH 6	13.4	0.0142	0.0043	1.3327	2.21	0.61[l]	36.9	64	60	33.5	34.5
DA	pH 6	5.4	0.0149	0.0043								
D	pH 6/Gdn·HCl	8.9	0.0175	0.0049	1.4430	2.26	0.41	32.8	27	13	38.7	45.0
DA	pH 6/Gdn·HCl	7.7	0.0134	0.0036								
D	GLOH	13.3	0.0141	0.0032	1.4070	2.30	0.61	35.8	ND	54	ND	34.9
DA	GLOH	6.1	0.0141	0.0042								
D	GLOH/urea	12.9	0.0086	0.0024	1.4400	2.25	0.59	35.1	ND	18	ND	45.2
DA	GLOH/urea	10.6	0.0279	0.0085								
D	GLOH/urea/DTT	12.5	0.0117	0.0028	ND	ND	0.57	35.1	ND	6	ND	55.5
DA	GLOH/urea/DTT	11.8	0.0180	0.0052								

[a] Asp(ENA) = N-Ac-Asp(ENA)$NHCH_3$; D = ENA-RNase A; DA = DNP-ENA-RNase A. [b] Solvents used were as follows: pH 2 = 50 mM Gly·HCl, pH 2; pH 4 = 100 mM potassium acetate, 185 mM KCl, pH 4; pH 4/Gdn·HCl = 100 mM potassium acetate, 185 mM KCl, 6 M Gdn·HCl, pH 4; pH 6 = H_2O, pH 6; pH 6/Gdn·HCl = H_2O, 6 M Gdn·HCl, pH 6; GLOH = 50% glycerol, 0.01 N HCl; GLOH/urea = 50% glycerol, 0.01 N HCl, 8 M urea; GLOH/urea/DTT = sample in 50% glycerol, 0.01 N HCl, and 8 M urea titrated to pH 8–8.5 with NaOH, 100 mM DTT added, and, after 2 h, sufficient HCl added to return the concentration to 0.01 N HCl. [c] Results of least-squares fit of the fluorescence decay kinetics with the equation $F(t) = \alpha e^{-t/\tau}$, where F is the true fluorescence decay, α is the preexponential factor, and τ is the lifetime. F is extracted from the observed response curve by a nonlinear least-squares procedure using iterative reconvolution (Grinvald & Steinberg, 1974). [d] Maximum deviation between the observed and calculated time-resolved fluorescence. [e] Root-mean square deviation between the observed and calculated time-resolved fluorescence. [f] Refractive index at the sodium D line. [g] Percent of energy transferred as calculated from fluorescence intensity measurements. [h] Percent of energy transferred using lifetime results. [i] Apparent donor–acceptor separation distance calculated from donor fluorescence intensity measurements when both distance distribution and Brownian motion are ignored. [j] Apparent donor–acceptor separation distance calculated from lifetime results when both distance distribution and Brownian motion are ignored. [k] The model compound Asp(ENA) had a high RMS deviation relative to ENA-RNase A. This may be due to an impurity, to internal quenching, or to an excited-state reaction. The lifetime of the major component may be smaller than the average lifetime by 0.5–1.0 ns. [l] This quantum yield was calculated by the comparative method with naphthalene as the standard (Berlman, 1971) and eq 5. The remaining quantum yields under other solvent conditions were calculated by comparison of the lifetime observed under those solvent conditions to the lifetime at pH 6, with eq 6 in the text.

nential and a more sophisticated analysis (Grinvald et al., 1972; E. Haas, C. A. McWherter, and H. A. Scheraga, work in progress) showed that there is actually a narrow distribution of interprobe distances in the native state. The deviation is small, and the heterogeneity in interprobe distance, while detectable, is not significant for the *conclusions of this work*. Furthermore, distributions of distances in the denatured states, manifested in the non-monoexponential decay of the ENA chromophore, are much less sensitive to uncertainties in the values of κ^2 (Haas et al., 1978a). Hence, the non-monoexponential decay of the ENA donor in the denatured states is a sensitive measure of purely distance distributions with no effect of the distributions of values of κ^2. This conclusion provides the basis for experiments currently in progress, determining intramolecular distance distributions by analysis of donor fluorescence decay curves.

Thus, the rotational diffusion about the bonds of the linker arms of ENA and DNP, and the probable effects of the mixed polarization of the electronic transitions, will randomize the relative orientations and make large errors unlikely. The results of the determination of J, Q, n, and R_0 are summarized in Table II.

The overlap of the emission spectrum of the donor with the absorption spectrum of the acceptor is a necessary condition for energy transfer between a donor–acceptor pair. Figure 7 illustrates an example of the overlap of the corrected emission spectrum of ENA-RNase A with the absorption spectrum of α-DNP-RNase A at pH 4. The emission band of ENA-RNase A was essentially identical with that of the model compound N-Ac-Asp(ENA)$NHCH_3$ (results not shown). As can be seen from Table II, the overlap integral was essentially a constant, ranging from 2.2×10^{-14} to 2.4×10^{-14} M^{-1} cm^3.

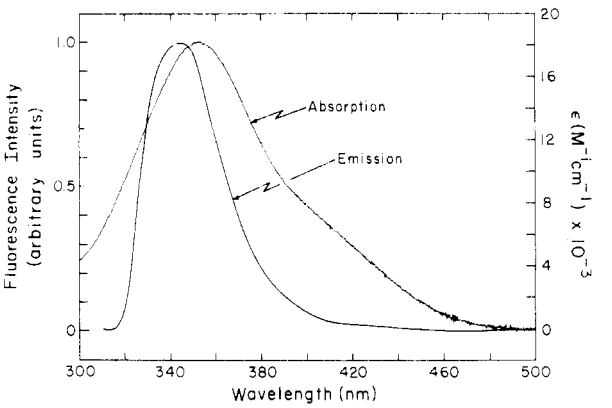

FIGURE 7: Corrected fluorescence emission spectrum of ENA-RNase A and absorption spectrum of α-DNP-RNase A. The corrected emission of the ENA group has a substantial overlap with the absorption of the DNP group, thus satisfying the requirement for energy transfer. The corrected spectrum is also used for calculations of Q, J, and R_0 (see Experimental Procedures). Bandwidth: excitation, 6 nm; emission, 8 nm.

This range is within the experimental uncertainties, which are limited in this case by the correction of the emission spectra. Similarly, Q and R_0 are relatively constant except when Gdn·HCl is present. The guanidine hydrochloride offers an alternative deexcitation pathway by serving as a collisional quencher. This was apparent in both the fluorescence intensity and lifetime measurements (Table II). The 30% decrease in the quantum yield of ENA-RNase A in the presence of 6 M Gdn·HCl reduced the value of R_0 from about 37 to 33 Å. The uncertainty in R_0 is more difficult to estimate. It depends on the uncertainty in J, Q, n, and κ^2. The uncertainty in Q is

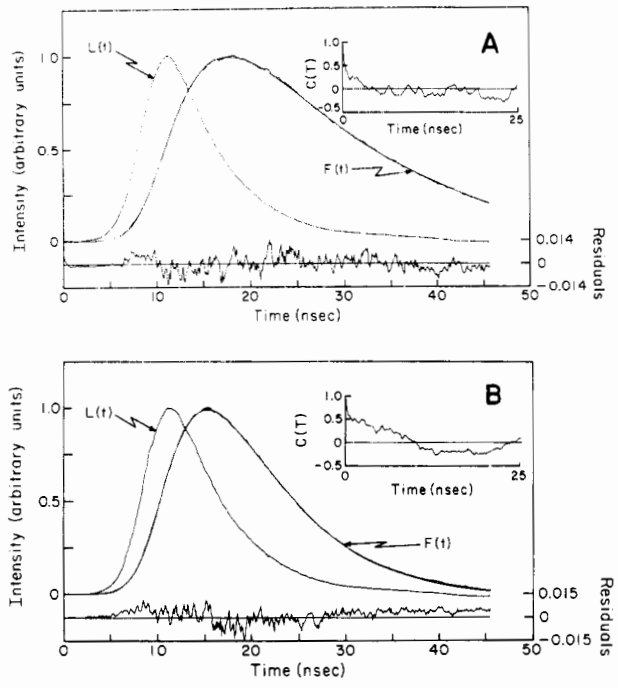

FIGURE 8: Fluorescence decay kinetics of ENA-RNase A and DNP-ENA-RNase A. (A) The time-resolved fluorescence decay of ENA-RNase A at pH 6 was measured in the instrument on the basis of the pulse sampling technique. A nitrogen flash lamp was used in conjunction with a double monochrometer to select the excitation pulse. The emission was observed above 345 nm by means of a Schott glass filter (WG 345) and a 3-mm piece of Corning Corex 7-60 glass. $L(t)$, lamp profile; $F(t)$, experimental decay of fluorescence. The smooth curve drawn over $F(t)$ is the calculated decay for the best fit with a monoexponential decay law. The noisy curve plotted below the lamp and fluorescence profiles, the residuals, is the difference between the observed and calculated fluorescence decay. The inset shows the autocorrelation of the residuals, $C(t)$. The nonlinear least-squares analysis gave a good monoexponential fit (RMS deviation 0.0043) of the data with a lifetime of 13.4 ns. The protein concentration was 13 μM. (B) Effect of energy transfer on the fluorescence decay kinetics. The time-resolved fluorescence of DNP-ENA-RNase A was measured under conditions identical with those of panel A. The observed shorter lifetime (5.4 ns, RMS deviation 0.0043) is evident from comparison with panel A. The protein concentration was 23 μM.

notoriously high because it depends on a standard value of questionable certainty and on the corrected emission spectra. The value of n is that of the bulk solvent (Moog et al., 1984). The effect of uncertainties in κ^2 has been widely discussed in the literature and would not be large for the reasons presented above. As many others before us, we argue that, because R_0 is determined by the sixth root of these factors, it will be moderately insensitive to their uncertainties. Thus, making the liberal, but arbitrary, estimate that κ^2, J, and Q were each high by 10%, we would calculate a slightly different value of R_0 of about 35 Å instead of 37 Å under native conditions. This translates into a 5% uncertainty in R_0.

Conformational Unfolding of the N-Terminal Region of RNase A and Estimates of Intramolecular Distances. Energy-transfer measurements were carried out by fluorescence intensity and lifetime measurements, with and without denaturants, and with and without disulfide bonds intact. The results are summarized in Table II.

The first issue is to compare the energy transfer determined by two independent methods, i.e., fluorescence intensity and lifetime measurements. Panels A and B of Figure 8 show the fluoresence decay kinetics of ENA-RNase A and DNP-ENA-RNase A, respectively, in H_2O at pH 6. The lifetimes determined from an analysis of the kinetics allow the determination of the efficiency of energy transfer with eq 3. The uncertainty in the lifetimes is estimated to be no more than 5% on the basis of the calibration of the instrument with anthracene as a standard (Badea & Brand, 1979). The energy transfer determined by intensity measurements has a larger uncertainity since it depends on two concentration measurements in addition to the two intensity measurements (eq 2). Lifetime measurements have the advantage of being independent of concentration and are not affected in these experiments by the innerfilter effect or reabsorption. In the five experiments in which a comparison of the two approaches was made, excellent agreement was observed in two cases (pH 4 and pH 6) in which the protein is not denatured and a single distance is observed. At pH 2, the results are very much at variance. However, the value of T_m of DNP-ENA-RNase A at pH 2 is 23 °C. Whereas the intensity measurements were carried out at 15 °C, the lifetime measurements were made at 22 °C. This means that the sample was partially unfolded in the lifetime measurement, hence the lower energy transfer. This conclusion is confirmed by the strong deviation from monoexponential decay observed in this measurement, as manifested by the high RMS deviations (Table II). These deviations show that multiple distances are present; i.e., the protein is partially unfolded. In the partially unfolded state, the fluorescence decay is not monoexponential because of the presence of multiple conformations. In that case, the average lifetime does not represent the quantum yield, and eq 3 and 6 are not applicable. Hence, the transfer efficiency calculated according to a monoexponential approximation of the decay curve $E(\tau)$ is lower than that calculated from the intensity $E(I)$. Moreover, $E(I)$ is also not a simple average over all distances. Detailed analysis of the intramolecular distance in unordered molecules as manifested by a multiexponential decay of donor fluorescence is beyond the scope of this paper and will be presented in a later paper. We conclude that, as found by others (Wu & Stryer, 1972), there is generally good agreement between the two techniques.

Inspection of Table II also reveals good agreement between the efficiency of energy transfer under folding conditions at pH 2, 4, and 6 (excluding the lifetime measurement at pH 2, see above). This implies agreement in distances measured at these three pHs since R_0 is relatively constant with pH. The average distance estimated under folding conditions is 35 ± 2 Å (using the same uncertainty estimate as made for R_0, see above). A more detailed analysis showed that the population of interprobe distances is slightly heterogeneous, exhibiting a narrow distribution (E. Haas, C. A. McWherter, and H. A. Scheraga, work in progress). In fact, this slight heterogeneity is expected, considering the flexibility of the probe linkage, and explains the slight deviation from monoexponential decay of the doubly labeled protein. Nevertheless, for the purpose of verifying the use of energy transfer in unfolding studies, the use of an average distance (especially considering the narrow width of the distribution) is appropriate. By use of the 1.45-Å RMS X-ray coordinates (Borkakoti et al., 1982) and by taking into account the labeling distribution, the average distance separating the α-amino nitrogen from the carboxylate carbon is 28 Å. In the Appendix, a simple model is described that takes into account the size of the linkages connecting the probes to the protein. The computed average interprobe distance of 36 Å is in excellent agreement with the experimental results reported here under folding conditions.

It is clear from a comparison of the data obtained under folding and unfolding conditions (Table II) that the efficiency of energy transfer can detect conformational unfolding.

Furthermore, the relatively specific labeling means that it is the N-terminal region that is unfolding. We propose that, by comparing conformational unfolding (or alternatively folding), as measured by energy transfer, with unfolding (or folding) measured by other techniques (say tyrosine absorbance), it may prove possible to study intermediates. Of course, if the intermediates have transient lifetimes, it may be necessary to develop techniques to trap them.

Finally, we note the trend observed when a denaturant was added and then the disulfide bonds were reduced. The efficiency of energy transfer in 50% glycerol [a potent stabilizer of native RNase A (Gekko & Timasheff, 1981)] decreases from 54 to 18% with the addition of 8 M urea and to 6% after reduction of the disulfide bonds with DTT.

A final cautionary note concerning the donor–acceptor distances reported in the presence of denaturant (Table II). It is our view that, at this level of analysis, these numbers are not meaningful. There is definitely an increase in distance on denaturation, as is well-known from hydrodynamic data [cf. Sela et al. (1957) and Tanford et al. (1966)]. However, because of the $1/r^6$ dependence of the transfer probability, the average distance measured will be weighted heavily toward short distances. A further complication arises from translational diffusion of the probes during the donor lifetime. Efforts to exploit this situation with the approach of Steinberg and co-workers (Haas et al., 1975, 1978b) are in progress. It is also of interest in this regard to note the proposal of Damjanovich and co-workers (Somogyi et al., 1984) to obtain distributions from steady-state measurements, although their approach has not yet been applied to *unfolded* proteins.

Further Discussion and Conclusions

We have labeled RNase A on the α-amino group with a nonfluorescent acceptor of electronic excitation energy. A donor probe was covalently attached to a carboxyl group in the vicinity of residue 50 (75% at Glu-49 and 25% at Asp-53 for both ENA- and DNP-ENA-RNase A). The two donor-labeled sites are close in sequence and have nearly the same separation distance from the acceptor site [27.6 and 28.5 Å (Borkakoti et al., 1982)]. Such a small difference would be unlikely to have a significant effect, given the uncertainties of the energy-transfer technique.

All of the derivatives prepared were fully active and underwent reversible thermal unfolding transitions. This means that these derivatives are able to maintain and readopt the native structure. We did, however, observe some changes in the quantitative aspects of denaturation. First, the masking of the carboxyl group lowered the value of T_m by about 5 °C at pH 2 and 4, in agreement with previous results (Riehm & Scheraga, 1966). Labeling at the α-amino group had no effect at pH 2 but resulted in a surprisingly dramatic decrease in the enthalpy change of the transition at pH 4. Apparently, there was also an entropic compensation since the value of T_m was changed very little.

The efficiency of energy transfer, determined by fluorescence intensity and lifetime measurements, varied from about 60% under folding conditions to 20% when the protein was unfolded with disulfides intact. Upon reduction, this decreased to roughly 5%. This range of variation is nearly ideal for maximum accuracy, with the energy-transfer technique. Thus, we were able to monitor conformational unfolding in the N-terminal region. The average interprobe separation distance (using the known labeling distribution) under folding conditions is estimated to be 35 ± 2 Å. The use of this average interprobe distance was appropriate because the distribution of distances is narrow (E. Haas, C. A. McWherter, and H.

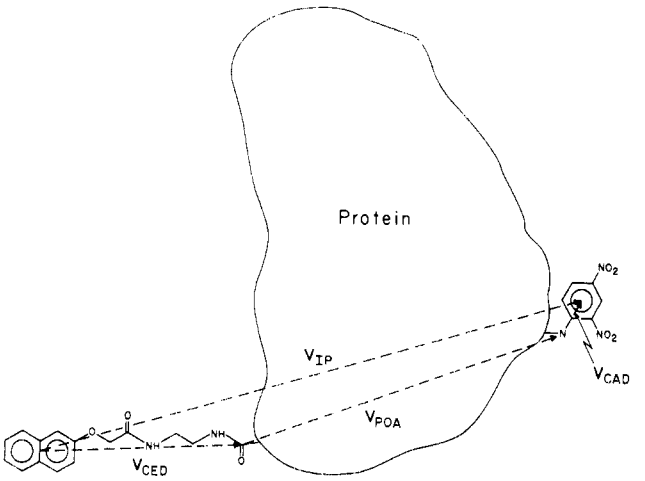

FIGURE 9: Schematic diagram illustrating the contribution of the probes to the interprobe distance.

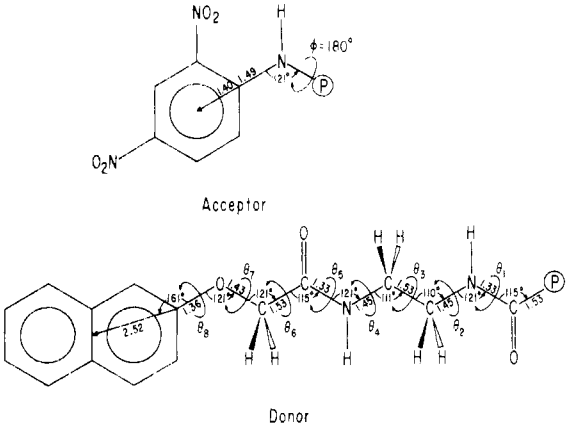

FIGURE 10: Notation and structural geometry of the probes. There are two peptide bonds (with partial double bond character) and six single bonds linking the donor to the protein (P).

A. Scheraga, work in progress). Considering the molecular dimensions of the probes, this is in good agreement with expectations based on the crystal structure and on a simple model of the conformational statistics of the donor probe linkage.

We have reported estimates of separation distances under unfolding conditions using *only* simple efficiency of energy-transfer measurements. It is our contention that such estimates are not meaningful because no information is available about the nature of the distribution in the unfolded molecules. Also, the relative diffusion of the two probes attached to the polypeptide chain is unknown, and hence, the effects of translational diffusion on the amount of energy transfer cannot be predicted. Thus, the distances that we report under unfolding conditions are difficult to interpret. The same comments apply to the recent work of Jullien and Garel (1983) and suggest the need for a more sophisticated analysis (Haas et al., 1975, 1978b). However, because our probes were in suitable positions with appropriate spectral properties, we were able to obtain interprobe distances that compare well with those expected from the known structure of the *native* protein. Under folding conditions, the decay of donor fluorescence from the doubly labeled protein is monoexponential. This satisfies an important requirement for the determination of distance distributions in the unfolded state by fluorescence decay measurements. Also, our derivatives specifically probe the N-terminal region of the molecule for which there is evidence of unfolding before the rate-limiting step (Lin et al., 1984, 1985). This establishes our derivatives as being suitable for

Table III: Relative Energies and Statistical Weights of the Rotational Isomeric States of the Donor Probe Linkage

bond rotational angle[a]	state[b]	energy, E_{ij}[c]	(stat wt)$_{ij}$[d]	q_i[e]
θ_1	180	0	1	1
θ_2	+60	0	1	
	−60	0	1	3
	180	0	1	
θ_3	+60	0.5	$e^{-0.5/(kT)}$	
	−60	0.5	$e^{-0.5/(kT)}$	$1 + 2e^{-0.5/(kT)}$
	180	0	1	
θ_4	+60	0	1	
	−60	0	1	3
	180	0	1	
θ_5	180	0	1	1
θ_6	+60	0	1	
	−60	0	1	3
	180	0	1	
θ_7	+60	0.5	$e^{-0.5/(kT)}$	
	−60	0.5	$e^{-0.5/(kT)}$	$1 + 2e^{-0.5/(kT)}$
	180	0	1	
θ_8	+90	0	1	2
	−90	0	1	

[a] Dihedral angles as depicted in Figure 10. These angles are defined by the atoms of the *backbone* of the linker and not by the pendant H and O atoms. [b] These are the rotational isomeric states of the corresponding bond rotational angles. The definition of the angles conforms to IUB–IUPAC recommendations. [c] Relative energy in kcal/mol. The ground-state energy is assigned to be zero. [d] The statistical weight given by the Boltzmann weighting factor, $e^{-E_{ij}/(kT)}$, where E_{ij} is the relative energy. [e] The bond partition function as defined in the text.

Table IV: Results of Calculations of the Average Interprobe Distance

		interprobe distance (Å)		
labeled residue[a]	direction of first bond[b]	individual average	labeled residue average[c]	overall average[d]
Glu-49	C^δ–O^ϵ (1)	36.8	36.5	36.1
Glu-49	C^δ–O^ϵ (2)	36.3		
Asp-53	C^γ–O^δ (1)	34.4	34.8	
Asp-53	C^γ–O^δ (2)	35.3		

[a] Residue labeled with donor probe. [b] Bond in the X-ray structure that defines the direction of the first bond of the donor probe in the calculation; 1 and 2 refer to the two different O^ϵ atoms of Glu-49 and likewise for the two O^δ atoms of Asp-53. [c] Average interprobe distance assuming equal probabilities for the direction of the first bond. [d] Overall average assuming equal probabilities for the direction of the first bond and taking into account 75% donor labeling at Glu-49 and 25% at Asp-53. For comparison, the value of $|\mathbf{V}_{POA}|$ is 27.6 Å between N^α and C^δ of Glu-49 and is 28.5 Å between N^α and C^γ of Asp-53.

the more sophisticated approaches (including the delineation of the folding/unfolding pathways, if these are sequential) alluded to above.

ACKNOWLEDGMENTS

We thank V. G. Davenport and M. Maytal for technical assistance, T. W. Thannhauser for nitrogen analysis and amino acid analysis, and G. Némethy for discussion of the rotational isomeric state model. We are indebted to Y. Konishi, Y. C. Meinwald, and E. R. Stimson for helpful discussions.

APPENDIX

Estimation of the Average Interprobe Distance Using Conformational Statistics of the Donor Probe Linkage. The energy-transfer technique determines the average distance between the center of the emission dipole (CED) of the donor and the center of the absorption dipole (CAD) of the acceptor (i.e., the average interprobe distance). An estimate of the consequences of the finite size of the donor and acceptor probes can be made by combining the conformational statistics of the donor probe linkage with geometrical considerations. Conformations of only the donor probe linkage need to be considered because rotation about the single bond connecting the acceptor to the protein does not change the distance[2] between the center of the acceptor chromophore and the nitrogen atom of the protein to which it is attached. The contributions of the donor and acceptor probes are combined with information from the X-ray structure to give an estimated average interprobe distance. For the purpose of this calculation, the conformation of the protein, including the side chains of Glu-49 and Asp-53, was taken to be fixed. The result of this calculation is compared with the experimental energy-transfer result obtained under conditions in which the protein adopts the native conformation.

The interprobe vector $\mathbf{V}_{IP}$ from the CED to the CAD can be represented as the sum of three vectors (see Figure 9):

$$\mathbf{V}_{IP} = \mathbf{V}_{CED} + \mathbf{V}_{POA} + \mathbf{V}_{CAD} \qquad (10)$$

where $\mathbf{V}_{CED}$ is a vector from the CED to the point of attachment (POA) of the donor to the protein, $\mathbf{V}_{CAD}$ is a vector from the POA of the acceptor to the protein to the CAD, and $\mathbf{V}_{POA}$ is a vector from the POA of the donor to that of the acceptor. The POA of the donor is either the C^δ of Glu-49 or C^γ of Asp-53, and the POA of the acceptor is the N^α of Lys-1. The average interprobe distance $\langle|\mathbf{V}_{IP}|\rangle$ is calculated according to the relation

$$\langle|\mathbf{V}_{IP}|\rangle = \sum_k (\text{stat wt})_k |\mathbf{V}_{IP}|_k / Z \qquad (11)$$

where $|\mathbf{V}_{IP}|_k$ is the magnitude of the interprobe vector when the donor probe linkage is in conformation k, $(\text{stat wt})_k$ is the statistical weight of conformation k, Z is the conformational partition function of the donor probe linkage, and the sum is taken over all conformations of the donor probe linkage. The vector $\mathbf{V}_{POA}$ is fixed in this calculation. Thus, $\mathbf{V}_{IP}$ varies only with the conformation of the donor probe linkage in this calculation.

The structural geometry and notation adopted for the probes are shown in Figure 10. Values for the bond lengths and bond angles were assigned on the basis of values published for compounds for similar structure. The vectors $\mathbf{V}_{CED}$, $\mathbf{V}_{POA}$, $\mathbf{V}_{CAD}$, and $\mathbf{V}_{IP}$ were calculated by standard techniques for manipulating molecular geometry [cf. Flory (1969)].

The donor probe linkage has six single bonds, each with partial rotational freedom. For this calculation, we have adopted the rotational isomeric state model [cf. Flory (1969)] in which rotation about each of the six single bonds is restricted to a few isomeric states. These states are assumed to be highly populated, low-energy states so that, to a reasonable approximation, the actual distribution of conformations is well represented with this restriction.

The isomeric states for the donor probe linkage along with their relative energies and statistical weights are shown in Table III. These values were assigned from conformational-analysis information for compounds containing similar structural elements.

The simplest model assumes that the population distribution among the states of each bond is independent of the other bonds in the linkage. It then follows that the conformational partition function can be factored into a product of individual partition functions, one from each bond, i.e.

$$Z = \prod_{i=1}^{8} q_i \qquad (12)$$

[2] Rotation about this bond, however, will change the orientation of the acceptor dipole since it is not collinear with the bond.

where q_i is the bond partition function of the ith bond and the product is formed from all the bonds of the linkage. The bond partition function is given by

$$q_i = \sum_j e^{-E_{ij}/(kT)} \quad (13)$$

E_{ij} is the relative energy of bond i when in state j. The sum is taken, of course, over all states j of bond i. Using eq 12 and 13 along with the information in Table III, it is straightforward to compute the conformational partition function:

$$Z = 54(1 + 2e^{-0.5/(kT)})^2 \quad (14)$$

At 298 K, the value of this expression is 187.6. The statistical weight of any given conformation is found by taking the product of the statistical weights of the bond states that define the conformation, i.e.

$$(\text{stat wt})_k = \prod_{i=1}^{8} (\text{stat wt})_{ij} \quad (15)$$

where $(\text{stat wt})_k$ is the statistical weight of a given conformation k, the product is taken over all bonds i, and $(\text{stat wt})_{ij}$ is the statistical weight assigned to bond i when it is in state j.

The average interprobe distance was calculated as follows. The interprobe vector $\mathbf{V}_{IP}$ was calculated for each conformation with eq 10 and standard techniques for the analysis of molecular geometry. The statistical weight of each conformation was calculated with eq 15 and the information in Table III. The interprobe vectors and the statistical weights of the conformations were then used, along with the conformational partition function, in eq 11 to calculate the average interprobe distance.

Table IV presents the results of four separate calculations of the interprobe distance. The distribution of donor labeling sites was accounted for by carrying out calculations for each of the two labeling sites. Each labeling site required a pair of calculations in order to allow the first bond of the donor probe to extend in the direction of either of the two equivalent carbon–oxygen bonds of the carboxylate group. Allowance of alternative first-bond directions is equivalent to allowing rotation about the C^{γ}–C^{δ} and C^{β}–C^{γ} bonds of Glu-49 and Asp-53, respectively. The average interprobe distance for the individual labeling sites was computed, assuming equal probability for the two alternative first-bond directions of the donor linkage. The overall average was calculated from the experimentally determined labeling distribution (75% at Glu-49 and 25% at Asp-53) and the labeled residue averages.

All of these results are in excellent agreement with the experimental results for the native protein (see Table VI). Both the choice of the first-bond direction and the labeling site had little effect on the average interprobe distance. Several points can be made concerning this calculation. First, it successfully uses a simple model that contained several approximations and assumptions; it did not attempt to model more complicated phenomena such as interaction between neighboring bonds, self-intersection, and penetration of the protein by the probe. The simple model provides an expedient way to compare the energy-transfer results with information from the X-ray structure. If self-intersection and exclusion of the probe by the protein had been taken into account, it is likely that the calculated average interprobe distance would have been *larger*. However, the experimentally determined average interprobe distance, with which this calculated value is compared, is not a simple population-weighted average. In addition to population weighting, there is weighting by the inverse sixth power of the distance that leads to *shorter* average distances in the experiment. If both effects (the increase due to self-exclusion and the decrease due to the inverse sixth power dependence) had been included in the calculation, they likely would have affected the result in opposite directions, tending to lead again to agreement between the calculated and experimental interprobe distances.

In summary, this simple model gives excellent agreement with experiment, and the larger distance expected with a more realistic model can still be accounted for when the underlying theory of energy transfer is considered.

Supplementary Material Available

Details of the preparation of the donor probe and the preparation, purification, and identification of the protein derivatives, including four tables and eight figures (35 pages). Ordering information is given on any current masthead page.

Registry No. NAA, 120-23-0; ENA, 100927-97-7; NAA-ONSu, 81012-92-2; HONSu, 6066-82-6; DNP, 99-65-0; RNase, 9001-99-4; Ac-Asp-$NHCH_3$, 36318-52-2; Ac-Asp(OBzl)-$NHCH_3$, 100927-98-8; Ac-Asp(ENA)-$NHCH_3$, 100938-72-5.

References

Acharya, A. S., & Vithayathil, P. J. (1975) *Int. J. Pept. Protein Res. 7*, 207–219.

Amir, D., Varshavski, L., & Haas, E. (1985) *Biopolymers 24*, 623–638.

Badea, M. G., & Brand, L. (1979) *Methods Enzymol. 61*, 378–425.

Berlman, I. B. (1971) in *Handbook of Fluorescence Spectra of Aromatic Molecules*, 2nd ed., p 330, Academic, New York.

Blackburn, P., & Moore, S. (1982) *Enzymes (3rd ed.) 15*, 317–433.

Borkakoti, N., Moss, D. S., & Palmer, R. A. (1982) *Acta Crystallogr., Sect. B: Struct. Crystallogr. Cryst. Chem. 38B*, 2210–2217.

Brandts, J. F. (1964) *J. Am. Chem. Soc. 86*, 4291–4301.

Brandts, J. F., & Hunt, L. (1967) *J. Am. Chem. Soc. 89*, 4826–4838.

Carraway, K. L., & Koshland, D. E., Jr. (1972) *Methods Enzymol. 25*, 616–623.

Carty, R. P., & Hirs, C. H. W. (1968) *J. Biol. Chem. 243*, 5244–5253.

Chen, R. F., & Bowman, R. L. (1965) *Science (Washington, D.C.) 147*, 729–732.

Chen, R. F., Edelhoch, H., & Steiner, R. F. (1969) in *Physical Principles and Techniques of Protein Chemistry* (Leach, S. J., Ed.) Part A, pp 204–208, Academic, New York.

Crook, E. M., Mathias, A. P., & Rabin, B. R. (1960) *Biochem. J. 74*, 234–238.

Denton, J. B., Konishi, Y., & Scheraga, H. A. (1982) *Biochemistry 21*, 5155–5163.

Fairclough, R. H., & Cantor, C. R. (1978) *Methods Enzymol. 48*, 347–379.

Flory, P. J. (1969) *Statistical Mechanics of Chain Molecules*, Chapter 3, Appendix B, Interscience, New York.

Garel, J.-R. (1976) *Eur. J. Biochem. 70*, 179–189.

Gekko, K., & Timasheff, S. N. (1981) *Biochemistry 20*, 4677–4686.

Grinvald, A., & Steinberg, I. Z. (1974) *Anal. Biochem. 59*, 583–598.

Grinvald, A., Haas, E., & Steinberg, I. Z. (1972) *Proc. Natl. Acad. Sci. U.S.A. 69*, 2273–2277.

Haas, E., Wilchek, M., Katchalski-Katzir, E., & Steinberg, I. Z. (1975) *Proc. Natl. Acad. Sci. U.S.A. 72*, 1807–1811.

Haas, E., Katchalski-Katzir, E., & Steinberg, I. Z. (1978a) *Biochemistry 17*, 5064–5070.
Haas, E., Katchalski-Katzir, E., & Steinberg, I. Z. (1978b) *Biopolymers 17*, 11–31.
Hazan, G. (1973) Ph.D. Thesis, The Feinberg Graduate School of the Weizmann Institute of Science.
Hazan, G., Grinvald, A., Maytal, M., & Steinberg, I. Z. (1974) *Rev. Sci. Instrum. 45*, 1602–1604.
Hermans, J., Jr., & Scheraga, H. A. (1961) *J. Am. Chem. Soc. 83*, 3283–3292.
Hirs, C. H. W., & Kycia, J. H. (1965) *Arch. Biochem. Biophys. 111*, 223–235.
Hirs, C. H. W., Moore, S., & Stein, W. H. (1960) *J. Biol. Chem. 235*, 633–647.
Hirs, C. H. W., Halmann, M., & Kycia, J. H. (1965) *Arch. Biochem. Biophys. 111*, 209–222.
Hundley, L., Coburn, T., Garwin, E., & Stryer, L. (1967) *Rev. Sci. Instrum. 38*, 488–492.
Jullien, M., & Garel, J.-R. (1983) *Biochemistry 22*, 3829–3836.
Kasha, M. (1948) *J. Opt. Soc. Am. 38*, 929–934.
Konishi, Y., & Scheraga, H. A. (1980) *Biochemistry 19*, 1308–1316.
Lakowicz, J. R. (1983) in *Principles of Fluorescence Spectroscopy*, Chapter 10, Plenum, New York.
Lakowicz, J. R., & Weber, G. (1980) *Biophys. J. 32*, 591–601.
Lin, S. H., Konishi, Y., Denton, M. E., & Scheraga, H. A. (1984) *Biochemistry 23*, 5504–5512.
Lin, S. H., Konishi, Y., Nall, B. T., & Scheraga, H. A. (1985) *Biochemistry 24*, 2680–2686.
Matheson, R. R., Jr., Dugas, H., & Scheraga, H. A. (1977) *Biochem. Biophys. Res. Commun. 74*, 869–876.
McWherter, C. A., Thannhauser, T. W., Fredrickson, R. A., Zagotta, M. T., & Scheraga, H. A. (1984) *Anal. Biochem. 141*, 523–537.
Moog, R. S., Kuki, A., Fayer, M. D., & Boxer, S. G. (1984) *Biochemistry 23*, 1564–1571.
Murdock, A. L., Grist, K. L., & Hirs, C. H. W. (1966) *Arch. Biochem. Biophys. 114*, 375–390.
Noel, R. J., & Hambleton, L. G. (1976) *J. Assoc. Off. Anal. Chem. 59*, 134–140.
Nozaki, Y. (1972) *Methods Enzymol. 26*, 43–50.
Richards, F. M., & Wyckoff, H. W. (1971) *Enzymes (3rd Ed.) 4*, 647–806.
Riehm, J. P., & Scheraga, H. A. (1966) *Biochemistry 5*, 99–115.
Sela, M., Anfinsen, C. B., & Harrington, W. F. (1957) *Biochim. Biophys. Acta 26*, 502–512.
Soleillet, P. (1929) *Ann. Phys. (Paris) 12*, 23–97.
Somogyi, B., Matko, J., Papp, S., Hevessy, J., Welch, G. R., & Damjanovich, S. (1984) *Biochemistry 23*, 3403–3411.
Steinberg, I. Z. (1971) *Annu. Rev. Biochem. 40*, 83–114.
Stryer, L. (1978) *Annu. Rev. Biochem. 47*, 819–846.
Taborsky, G. (1959) *J. Biol. Chem. 234*, 2652–2656.
Tanford, C., Kawahara, K., & Lapanje, S. (1966) *J. Biol. Chem. 241*, 1921–1923.
Thannhauser, T. W., McWherter, C. A., & Scheraga, H. A. (1985) *Anal. Biochem. 149*, 322–330.
Thomas, D. D. (1978) *Biophys. J. 24*, 439–462.
Valeur, B., & Weber, G. (1977) *Chem. Phys. Lett. 45*, 140–144.
Valeur, B., & Weber, G. (1978) *J. Chem. Phys. 69*, 2393–2400.
Weber, G., & Teale, F. W. J. (1957) *Trans. Faraday Soc. 53*, 646–655.
Wlodawer, A., Bott, R., & Sjolin, L. (1982) *J. Biol. Chem. 257*, 1325–1332.
Wu, C. W., & Stryer, L. (1972) *Proc. Natl. Acad. Sci. U.S.A. 69*, 1104–1108.